

Retinal optic flow during natural locomotion

Jonathan Samir Matthis^{1,*}, Karl S Muller², Kathryn Bonnen³, Mary M Hayhoe²,

¹ Department of Biology, Northeastern University, Boston, MA, USA

² Center for Perceptual Systems, University of Texas at Austin, TX, USA

³ Center for Neural Science, New York University, New York, NY, USA

* j.matthis@northeastern.edu

NON-PEER-REVIEWED DRAFT MANUSCRIPT – SUBJECT TO CHANGE

Abstract

We examine the ways that the optic flow patterns experienced during natural locomotion are shaped by the movement of the observer through their environments. By recording body motion during locomotion in natural terrain, we demonstrate that head-centered optic flow is highly unstable regardless of whether the walker's head (and eye) is directed towards a distant target or at the ground nearby to monitor foothold selection. In contrast, VOR-mediated retinal optic flow has stable, reliable features that may be valuable for the control of locomotion. In particular, we found that a walker can determine whether they will pass to the left or right of their fixation point by observing the sign and magnitude of the curl of the flow field at the fovea. In addition, the divergence map of the retinal flow field provides a cue for the walker's overground velocity/momentum vector in retinotopic coordinates, which may be an essential part of the visual identification of footholds during locomotion over complex terrain. These findings casts doubt on the assumption that accurate perception of heading direction requires correction for the effects of eccentric gaze, as has long been assumed. The present analysis of retinal flow patterns during the gait cycle suggests an alternative interpretation of the way flow is used for both perception of heading and the control of locomotion in the natural world.

Clickable Video Links (Click here for a playlist of all videos)

<https://www.youtube.com/playlist?list=PLWxH2Ov17q5HRHVngfuMgMZn8qfOivMaf>

- Video 1.** Gaze Laser Skeleton – Video (Full Speed) – Free Walking – Raw (See Figure 1)
- Video 2.** Gaze Laser Skeleton – Video (1/4 Speed) – Free Walking – Optic Flow Vectors
- Video 3.** Gaze Laser Skeleton – Video (1/4 Speed) – Free Walking – Optic Flow Streamlines
- Video 4.** Sim. Eye Trajectory – Sim. Retinal Flow – Fixation Aligned with Path
- Video 5.** Sim. Eye Trajectory – Sim. Retinal Flow – Fixation to Left of Path
- Video 6.** Sim. Eye Trajectory – Sim. Retinal Flow – Fixation to Right of Path
- Video 7.** Sim. Eye Trajectory – Sim. Retinal Flow – Vertical Sin Wave
- Video 8.** Sim. Eye Trajectory – Sim. Retinal Flow – Horizontal Sin Wave
- Video 9.** Sim. Eye Trajectory – Sim. Retinal Flow – Corckscrew
- Video 10.** Gaze Laser Skeleton – Sim. Retinal Flow – Ground Looking
- Video 11.** Gaze Laser Skeleton – Video (Full Speed) – Rocky Terrain – Raw
- Video 12.** Gaze Laser Skeleton – Video (1/4 Speed) – Rocky Terrain – Optic Flow Streamlines
- Video 13.** Gaze Laser Skeleton – Sim. Retinal Flow – Rocky Terrain
- Video 14.** Quadcopter Gimbal – Video (Full Speed) – Optic Flow Streamlines

1 Introduction

Movement of the body through space creates image motion on the retinae. In the absence of eye movements, an observer moving through a structured environment will experience a pattern of radial expansion centered on a location, called the Focus of Expansion (FoE), that specifies the current heading direction (Gibson, 1950, 1979). Subsequent work showed that observers are able to judge their heading in simulated flow fields with very high accuracy, on the order of 1-2 degrees of error (Warren, 1988). As a consequence of this observation, together with a large body of related work, it became generally accepted that the optic flow patterns arising from linear translation are used by observers to control their direction of heading during locomotion (see reviews by Lappe, Bremmer, & van den Berg, 1999; Warren, 2007; Li & Cheng, 2013; Britten, 2008). Similarly, this idea has dominated the interpretation of neural activity in motion-sensitive areas of visual cortex such as MST and VIP, areas that respond selectively to optic flow stimuli and are thought to underlie both human and monkey heading judgments (Britten, 2008; A. Chen, Gu, Liu, DeAngelis, & Angelaki, 2016; X. Chen, DeAngelis, & Angelaki, 2013; Duffy & Wurtz, 1991; Morrone et al., 2000; Wall & Smith, 2008; Bremmer, Churan, & Lappe, 2017).

A complication of this simple strategy, however, is that moving observers move their eyes. Nearly all vertebrates utilize a “saccade and fixate” strategy whereby gaze is moved rapidly to a new location and then stabilized by reflexes such as the Vestibular Ocular Reflex (VOR), in order to minimize image blur (Dietrich & Wuehr, 2019; Land, 2018). The optical consequences of eccentric gaze during locomotion were recognized in Gibson’s original treatment (e.g. Gibson, 1950, Figure 57), but the emphasis there and in subsequent research on the topic was on how the observer could decompose retinal flow into the rotational component caused by the eye movement and the eye-movement-free (head-centered) translational component assumed to specify locomotor heading. Recovering heading direction from retinal optic flow during a fixation been referred to as the “rotation problem” (Britten, 2008), or the “eye movement problem” (Warren & Hannon, 1990).

This issue has been central to much of the research on optic flow. Experimental on this issue typically involve head-fixed, seated observers making judgements about their heading inferred from fields of moving dots that simulate constant velocity forward motion¹. This task is generally performed either while maintaining central fixation, while fixating a moving probe within the dot field, or while maintaining central fixation on a moving dot field that is altered to simulate the optical effects of an eye rotation (Lappe et al., 1999; Li & Warren, 2004; Paolini, Distler, Bremmer, Lappe, & Hoffmann, 2000; Royden, Banks, & Crowell, 1992; Royden, Crowell, & Banks, 1994). The fact that heading judgements remain accurate in all of these conditions led to the conclusion that subjects must be correcting for the optical effects of their own eye movements in order to recover the stable, head-centered, translational optic flow and thus to determine heading.

However, there are at least two important issues to consider in understanding the role of optic flow in the control of locomotion – one concerning the stimulus and the

¹Literature on this topic often refers to fixations on the ground during locomotion as “pursuit” eye movements. This is accurate for fixation of a moving probe on a computer-screen, but the eye rotation during ground fixation during real locomotion is not smooth pursuit, which occurs when an observer fixates an object that is moving independently of the background. Fixation of a point on the ground during locomotion is driven by reflexes such as VOR that serve to stabilize the retinae relative to the external world. Although the kinematics of the eye during smooth pursuit and VOR mediated fixation are similar, they have very different neural and evolutionary underpinnings (Lappi, 2016).

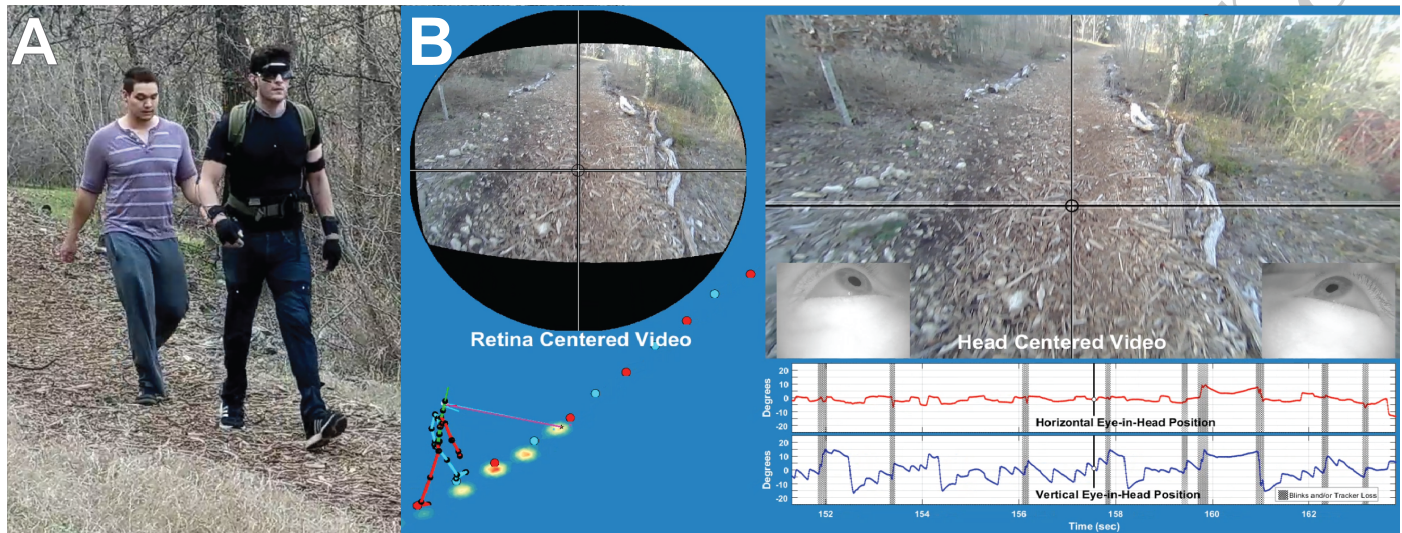


Figure 1. The data collection setup. (A) shows the subject walking in the Woodchips terrain wearing the Pupil Labs binocular eye tracker and Motion Shadow motion capture system. Optometrist roll-up sunglasses were used to shade the eyes to improve eye tracker performance. (B) shows a sample of the data record, presented as a sample frame for Video 1. On the right is the view of the scene from the head camera, with gaze location indicated by the crosshair. Below that are the horizontal and vertical eye-in-head records, with blinks/tracker losses denoted by vertical gray bars. The high velocity regions (steep upwards slope) show the saccades to the next fixation point, and the lower velocity segments (shallow downwards slope) show the vestibular ocular reflex component that stabilizes gaze on a particular location in the scene as the subject moves towards it, resulting a characteristic saw-tooth appearance for the eye signal (without self-motion and VOR these saccades would exhibit a more square-wave like structure). On the left, the stick figure shows the skeleton figure reconstructed from the Motion Shadow data. This is integrated with the eye signal which is shown by the blue and pink lines. The representation of binocular gaze here shows the gaze vector from each eye converging on a single point (the mean of the two eyes). The original ground intersection of the right and left eye is shown as a magenta or cyan dot (respectively, more easily visible in Video 1). The blue and red dots show the foot plants recorded by the motion capture system. The top left figure shows the scene image centered on the point of gaze reconstructed from the head camera as described in the Methods section.

other concerning the interpretation of the observations. The stimulus-related issue is that the simulated self-motion in the experiments is almost always based on constant velocity, straight-line movement. These stimuli produce a strong sense of self-motion, orvection, and are a reasonable approximation to the airplanes, automobiles, and gliding birds that were the basis of Gibson's original insights. However, they bear little resemblance to natural locomotion, which generates rhythmic translation and rotation profiles of the head in space, peaking at approximately 2Hz, which is the natural period of footsteps (Menz, Lord, & Fitzpatrick, 2003; Kavanagh & Menz, 2008). This means that the momentary heading direction varies through the gait cycle, creating a complex pattern of flow on the retina. In what follows, we will explore the way that the natural translation and acceleration patterns of the head during human locomotion shape optic flow in ways that are not usually considered in the literature.

The second, related, issue is how the experimental results might provide insights into how human walkers use optic flow to control locomotor heading. The key assumption behind work on the rotation problem is that removal of the rotational component of flow caused by a stabilizing eye movement will return a translational flow field with a stable FoE that may be used to guide heading. If natural oscillations of the head are enough to destabilize head-centered (eye-movement free) flow fields, then locomotor control strategies that rely on a stable FoE become untenable. Wann and Land (2000) argued that it is not necessary to recover heading direction in order to control steering towards a goal, since diagnostic patterns are available in the retinal flow field to control the path. The geometric relation between retinal optic flow patterns and particular relations between gaze and translation direction was worked out in a series of papers by Koenderink and van Doorn (e.g. Koenderink, 1986; Koenderink & van Doorn, 1976, 1984), and this work also suggested that retinal flow patterns might be informative. Additionally, steering towards a goal can use visual direction information, so recovery of heading from the retinal optic flow may be unnecessary (Rushton, Harris, Lloyd, & Wann, 1998; Rogers & Dalton, 1999). Subsequent work, however, supported the use of instantaneous direction of travel from optic flow to control heading (Warren, Kay, Zosh, Duchon, & Sahuc, 2001; Li & Cheng, 2013; Li & Niehorster, 2014; R. Chen, Niehorster, & Li, 2017).

Part of the difficulty in understanding the role of optic flow in human locomotion is that most studies on the topic utilize computer-screen-based "simulated self-motion" that lacks the complexity of actual locomotion. The gait-induced instabilities of the head and the complex, terrain-dependent patterns of eye movements during natural locomotion will determine the actual flow patterns on the retina, and these patterns will be different from those observed during passive translation such as in a moving vehicle. Because of the difficulty of measuring both the eye and body movements outdoors and measuring the consequent retinal motion, these patterns have not previously been measured, so the actual optic flow induced by locomotion in the natural world has not been examined. Therefore, a goal of this paper was to measure eye and body movements during natural locomotion and to use this data to calculate the resulting optic flow patterns. By characterizing the optic flow stimulus experienced during natural locomotion, we may gain a greater insight into the ways that the nervous system may exploit these signals for the control of action.

1.1 Retinal and head-centered optic flow during real-world locomotion

To explore the role of optic flow in the context of natural locomotion, we measured eye and body movements, and recorded video data from a head mounted camera as subjects walked through natural environments. We make two main points that call for a re-evaluation of the role of head-centered optic flow in controlling heading. First, we show that head-centered optic flow (optic flow that is unaffected by eye movements) is highly unstable as a consequence of natural head movements during the gait cycle. These instabilities occur no matter where the subject is looking and regardless of task. This makes it unlikely that the focus of expansion is used to control heading during locomotion. Secondly, we will show that a richer and more stable source of information about heading with respect to the local surroundings can be derived directly from the retinal flow fields that arise from fixations on the ground plane during locomotion. Thus, we need to rethink the role of optic flow for the control of locomotion. We argue that rather than thinking of eye movements as a problem to be solved, we should examine the ways that the gaze stabilization regularizes retinal flow in ways that make available critical visual motion information for control of the body with respect to the local surroundings (Glennerster, Hansard, & Fitzgibbon, 2001). We show that this structure of fixation-mediated retinal optic flow provides a rich and robust source of information that is directly relevant to locomotor control without the need to subtract out or correct for the effects of eye rotations.

We recorded subjects walking in natural environments while wearing a full-body, IMU-based motion capture suit (Motion Shadow, Seattle, WA, USA) and a binocular eye tracker (Pupil Labs, Berlin, Germany). Data from the two systems were synchronized and spatially calibrated using methods similar to those described in Matthis, Yates, and Hayhoe (2018). This generated a data set consisting of spatiotemporally aligned full-body kinematic and binocular gaze data (sampled at 120Hz per eye), as well as synchronized first-person video from the head-mounted camera of the eye tracker (100 deg. diagonal, 1080p resolution, 30Hz). The integrated data are shown by the skeleton and gaze vectors in Figure 1B and Video 1. Subjects walked in two different environments: a flat tree-lined trail consisting of mulched woodchips shown in Figure 1 (selected because it was highly visually textured, but flat enough that foot placement did not require visual guidance), and a rocky, dried creek bed, where successful locomotion requires precise foot placement (This was the same terrain used in the ‘Rough’ condition of Matthis et al. (2018)). Subjects walked the woodchips path while completing one of three experimental tasks: “Free Viewing,” where subjects were asked to walk while observing their environment with no explicit instruction; “Ground Looking” where subjects were asked to look at the ground at a self-selected distance ahead of them (intended to mimic gaze behavior on the rocky terrain without the complex structure or foothold constraints)²; “Distant Fixation”, wherein subjects were asked to maintain fixation on a self-selected distant target that was roughly at eye height (this condition was intended to most closely mimic psychophysical tasks that have been employed to explore the role of optic flow in the control of locomotion, (e.g. Lappe et al., 1999; Paolini et al., 2000; Royden et al., 1992; Warren & Hannon, 1990). Walking over the rocky terrain (labelled “Rocks”) was demanding

²Note that although previous research has suggested that walkers may engage in “travel gaze” during locomotion (where gaze is “visually anchored in the front of the individual and carried along by the whole body movement (Patla & Vickers, 2003)”), this behavior is not physiologically possible due to gaze stabilization reflexes such as the VOR and OKN. As such, the Ground Looking condition actually consisted of a series of brief fixations and small saccades to keep gaze roughly a fixed distance ahead of the walker.

enough that subjects were not given instructions other than to walk from the start to
the end position at a comfortable pace.

2 Optic flow during real-world locomotion

2.1 Head-centered optic flow is not stable during natural locomotion

Existing literature on the topic on the role of optic flow in the control of locomotion suggests that walkers control their heading by “keeping the focus of expansion in the direction one must go (Gibson, 1950, pg128),” and that walkers use the FoE to steer when walking in visually structured environments (Warren et al., 2001). As described above, if the observer looks away from the direction of heading, a rotational component is introduced to the flow pattern on the retina. To solve this problem, extensive research has suggested that observers can recover the direction of heading by subtracting out the resulting rotational component using either knowledge of eye position or information in the flow pattern itself and it is thought that the recovered heading direction is then used to control direction of steering towards a goal (e.g. Warren, 2007; Royden et al., 1992, 1994; Lappe et al., 1999; Li & Warren, 2004; Paolini et al., 2000). This visual control strategy implicitly assumes that the focus of expansion within the eye-movement-free head centered optic flow is stable enough to provide accurate estimate of heading (Li & Warren, 2004). To examine this hypothesis, we first ran the videos from the head-mounted camera of the eye trackers through a computational optic flow estimation algorithm (DeepFlow, Weinzaepfel, Revaud, Harchaoui, & Schmid, 2013), which provides an estimate of image motion for every pixel of each frame of the video (Video 2). We then tracked the focus of expansion (FoE) within the resulting flow fields using a novel method inspired by computational fluid dynamics (See Methods. This analysis provides an estimate of the FoE location in head-centered coordinates for each video frame (Video 3). Given that research on the “rotation problem” focuses on strategies for removing the effects of eye movements on retinal optic flow, these head-centered optic flow estimates should be expected to provide a viable estimate of the walker’s direction of heading.

We found that the head-centered optic flow pattern is highly unstable, rarely corresponds to the walker’s direction of travel, and never lies in a stable location for more than a few frames at a time. While the consequences of gait-induced oscillations on the focus of expansion have been considered in the literature (van den Berg, 2000), they have not been explicitly examined and typically referred to as “jitter” and assumed to be a minor factor (e.g. van den Berg & Beintema, 2000; Nakamura, Palmisano, & Kim, 2016; Palmisano, Gillam, & Blackburn, 2000). In contrast, we find that even with the wide field of view camera (100 degree diagonal), the translation of the FoE is such that it often falls off screen, and is only on screen for an average of 40.6 +/- .06% of frames across each of the 4 conditions. On each frame of the recording, the FoE moves rapidly across the camera’s field of view at very high velocities, with a modal velocity across conditions of about 255 deg per sec. Note that this analysis is entirely based on the (securely) head-mounted camera and does not rely on the IMU measurements. To ensure that this instability is not just a consequence of the video-based technique, we also measured the FoE in the video of a gimbal-stabilized quadcopter camera drone (DJI Phantom 4, Nanshan, Shenzhen, China) and found it to be stable (See Methods and Video 14). Thus, it seems that this method is capable of identifying a stable FoE within a video recording, so we feel confident that

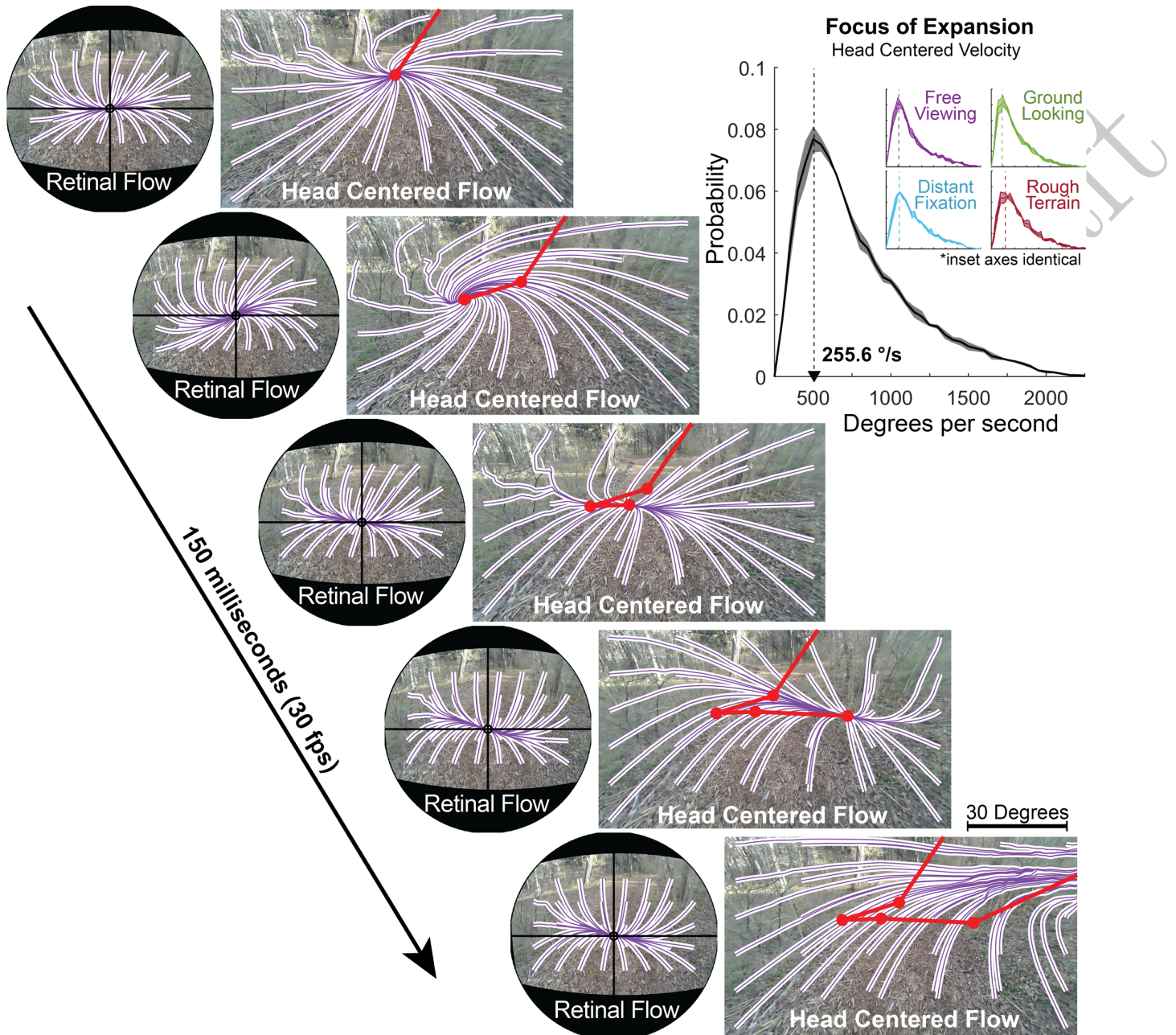


Figure 2. Retinal vs Head-Centered Optic flow. Optic flow patterns (down-sampled) for a sequence of 5 video frames from Video 3, altered for visibility in print. Head centered flow shows optic flow in the reference frame of the head mounted “world” camera, and represents optic flow free from the effects of eye movements. Retinal flow shows optic flow in the reference frame of a spherical pinhole camera stabilized on the subject’s fixation point. Purple and white lines show the integral curves of the measured flow fields, determined by using the streamlines2 function in Matlab to make a grid of particles drift along the negation of the flow fields measured by the DeepFlow optical flow detection algorithm in OpenCV. The red trace shows the movement of the head-centered FoE moving down and to the right across the 5 frames. Note the stability of the retina-centered flow in contrast. The inset shows the probability of finding a FOE velocity on an given video across all conditions (black histogram), as well as split by condition (colored insets). The thick line shows the mean across subjects, and shaded regions show ± 1 standard error.

instability in the head-centered FoE is genuine. 182

The instability of the head-centered FoE can be seen in Figure 2, which shows 183
the head-centered optic flow for a sequence of 5 frames. The red line traces the move- 184
ment of the FoE over the 5 frames (150ms). The inset in the figure shows the veloc- 185
ity distribution for the FoE, where the average of the 4 conditions is shown in black, 186
and the distributions for the different conditions is shown by the colored curves. Note 187
that the instability of the FoE is little affected by either the terrain (rocks or wood- 188
chips) or by subject's choice of gaze point, which is linked with head posture. The 189
instability of the head-centered FoE is also clearly demonstrated in Video 3, which 190
shows the integral lines of the optic flow fields shown in Video 2 with the FoE on each 191
frame denoted by a yellow star. This unexpected lack of stability clearly contradicts 192
the implicit assumption of much of the psychophysical experiments on this topic that 193
the head trajectory during locomotion can be approximated by constant velocity 194
straight line motion (occasionally with added 'jitter' (Palmisano et al., 2000)), and 195
indicates that the traditional story of how the FoE is used control steering towards a 196
goal is untenable on the basis of the naturally occurring visual stimulus. In contrast, 197
the retinal flow patterns shown in Figure 2 change only modestly over time as a con- 198
sequence of the gaze stabilization strategy of the oculomotor system. This suggests 199
that gaze stabilization may be an important component in understanding the use 200
of optic flow patterns, rather than a complicating factor as has been long assumed 201
(Britten, 2008). When gaze is properly stabilized on a location in the world during 202
locomotion, the result will always be a pattern of radial expansion combined with 203
rotation, centered on the point of fixation, this suggests that the critical feature is the 204
structure of the retinal flow pattern itself rather than the FoE. In what follows, we 205
explore some of the task relevant features of retinal flow below. 206

2.2 Head velocity oscillations during natural locomotion 207

The instability of head-centered optic flow arises from the natural oscillations of 208
the head during natural locomotion. A walker's head undergoes a complex, repeating 209
pattern of velocity throughout the gait cycle, as shown in Figure 3. Although the 210
vestibulocollic and spinocollic reflexes result in some damping of head acceleration 211
in the Anterior/Posterior and Medial/Lateral directions (note the flattening of the 212
acceleration profile between the hips, chest, and head in these dimensions), no such 213
damping appears to occur in the vertical direction, most likely because it would in- 214
terfere with the efficient exchange of potential and kinetic energy inherent in the 215
inverted pendulum dynamics of the bipedal gait cycle (Donelan, Kram, & Kuo, 2001; 216
Kuo, 2007; Mochon & McMahon, 1980). As a result, a walker's head undergoes a 217
continuously changing phasic velocity profile over the course of each step (see yellow 218
vector and trace in Video 3, which shows the velocity vector of the walker's eyeball 219
center at each frame of the recording). The peak magnitude of these velocity oscilla- 220
tions (particularly in the vertical dimension) is approximately half the walker's overall 221
walking speed, as shown in the Figure. 222

These variations in head velocity (Figure 3) and the accompanying rotations 223
(Supplemental Figure 4) throughout the gait cycle are the reason why the head- 224
centered FoE moves at such high velocities across a walker's visual field. The loca- 225
tion of the FoE at any given moment will be defined by the head's velocity vector 226
(Longuet-Higgins & Prazdny, 1980), so changes in that vector will lead to changes in 227
the FoE's location in the visual field. Furthermore, because the FoE arises from the 228
visual motion of objects in the walker's field of view, the linear velocity of the FoE 229
in the viewing plane of the walker will be determined by the angular variations in 230

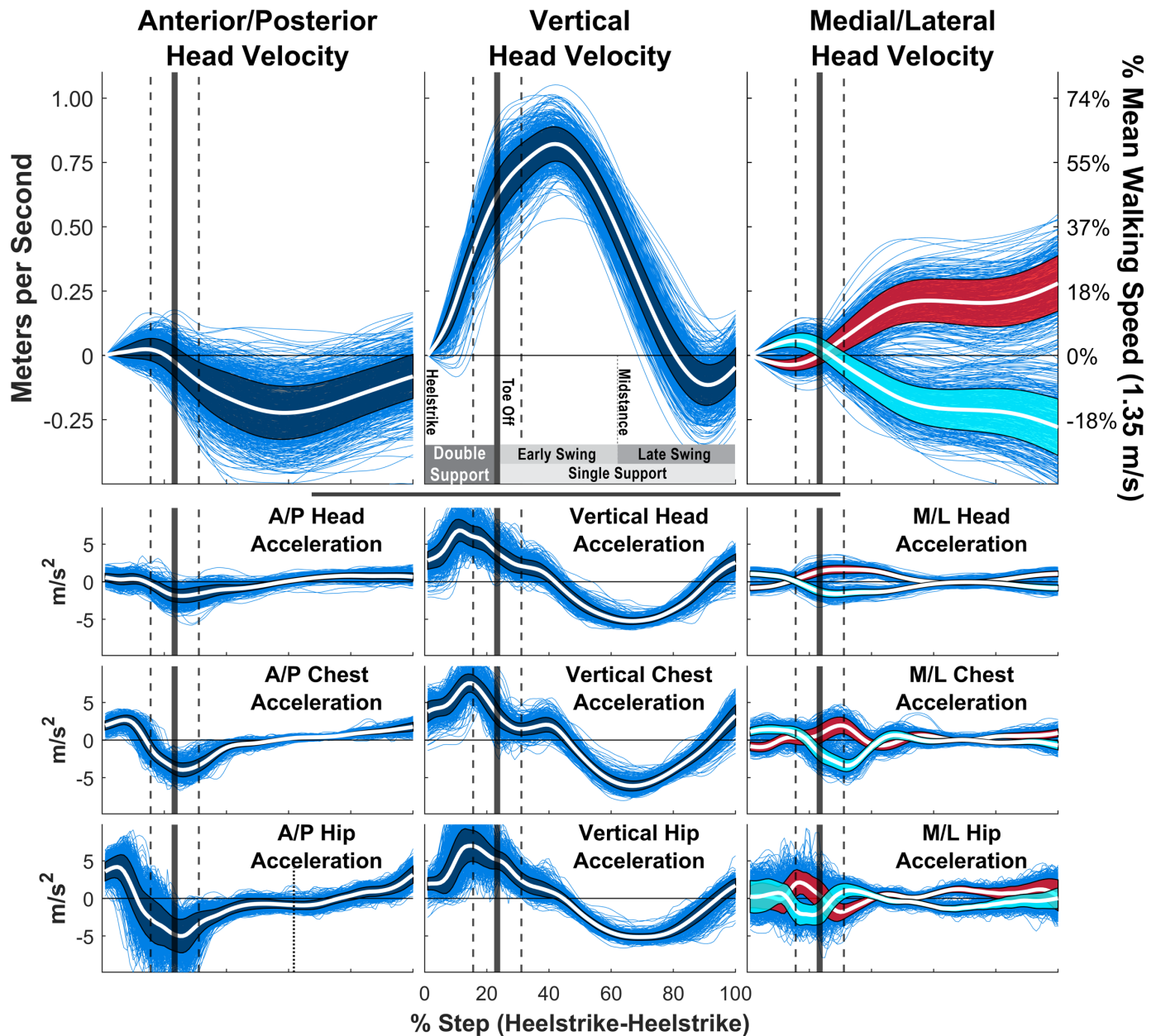


Figure 3. Head Velocity and Acceleration during locomotion. Head velocity and head/chest/hips acceleration patterns of a single representative subject walking in the "Distant Fixation" condition (where they walk while maintaining fixation on a point far down their path). Each blue trace is the velocity or acceleration trace for a single step, normalized for the time period from heel-strike to the subsequent heel-strike. The white line shows the mean and the shaded region is ± 1 standard deviation. Right and Left steps were computed separately for the Medial/Lateral data, and are shown in red and cyan respectively. The vertical solid lines show mean toe-off time, with the vertical dashed lines showing ± 1 standard deviation. Other subjects and conditions can be found in the Supplemental Information [NEEDS DONE].

the walker's head velocity vector projected onto the visible objects within walker's environment. Consequently, small angular changes in the walker's head velocity result in rapid, large scale movements in the FoE on the walker's image plane.

3 Simulated retinal flow

Head oscillations during walking render head-centered optic flow too unstable for use as a visual cue for locomotor heading. However, it is useful to examine the visual motion incident on the walker's retina, since this is the signal that is directly available to the visual system. To investigate the structure of the retinal motion patterns, or retinal flow, we used the walkers' recorded gaze and kinematic data to geometrically simulate the flow patterns experienced during natural locomotion.

These simulations of retinal flow utilize a spherical pinhole camera model of the eye (Figure 4). The spherical eye maintains 'fixation' on a point on the ground, while a grid of other ground points is projected through the pupil and onto the back of the spherical eye. The locations of these projected ground points on the retina are tracked frame by frame to calculate simulated retinal optic flow. The location of this eyeball can be set to maintain fixation while following an arbitrary trajectory through space to determine the structure of retinal optic flow during various types of movement (Videos 4-9). In addition, this model of the eye can be set to follow the trajectory of walker's eyes as they walked in natural terrain (Videos 10 and 13) in order to estimate retinal motion experienced during natural locomotion, without the complicating elements associated with the real-world video recordings (see Methods for details).

3.1 Retinal cues for the control of locomotion

We find several features of the resulting retinal flow patterns that could be powerful cues for the visual control of locomotion. ³ By definition, stabilization of gaze during fixation nulls visual motion at the fovea, so the basic structure of retinal optic flow will always consist of outflowing motion centered on the point of fixation. The retinal motion results from the translation and rotation of the eye in space, carried by the body and the walker holds gaze on a point on the ground during forward movement.

3.1.1 Foveal curl provides a cue for locomotor head relative to the fixation point

When a walker fixates a point that is aligned with their current velocity vector, the resulting retinal flow field has no net rotation at the fovea (Figure 5A, Video 4). However, fixation of a point that is off of their current trajectory results in a rotating pattern of flow around the fovea that may be quantified by calculating the curl of the retinal vector field. Fixation of a point that is to the left of the current path results in counter-clockwise rotation (Figure 5B, Video 5), while fixation to the right of the current trajectory results in clockwise rotation around the fovea (Figure 5C, Video

³This section relies heavily on the notions of *Curl* and *Divergence* from the field of vector calculus. For an excellent intuitive introduction to this topic we recommend [this YouTube video by 3Blue1Brown]

Spherical Pinhole Camera Eye Model

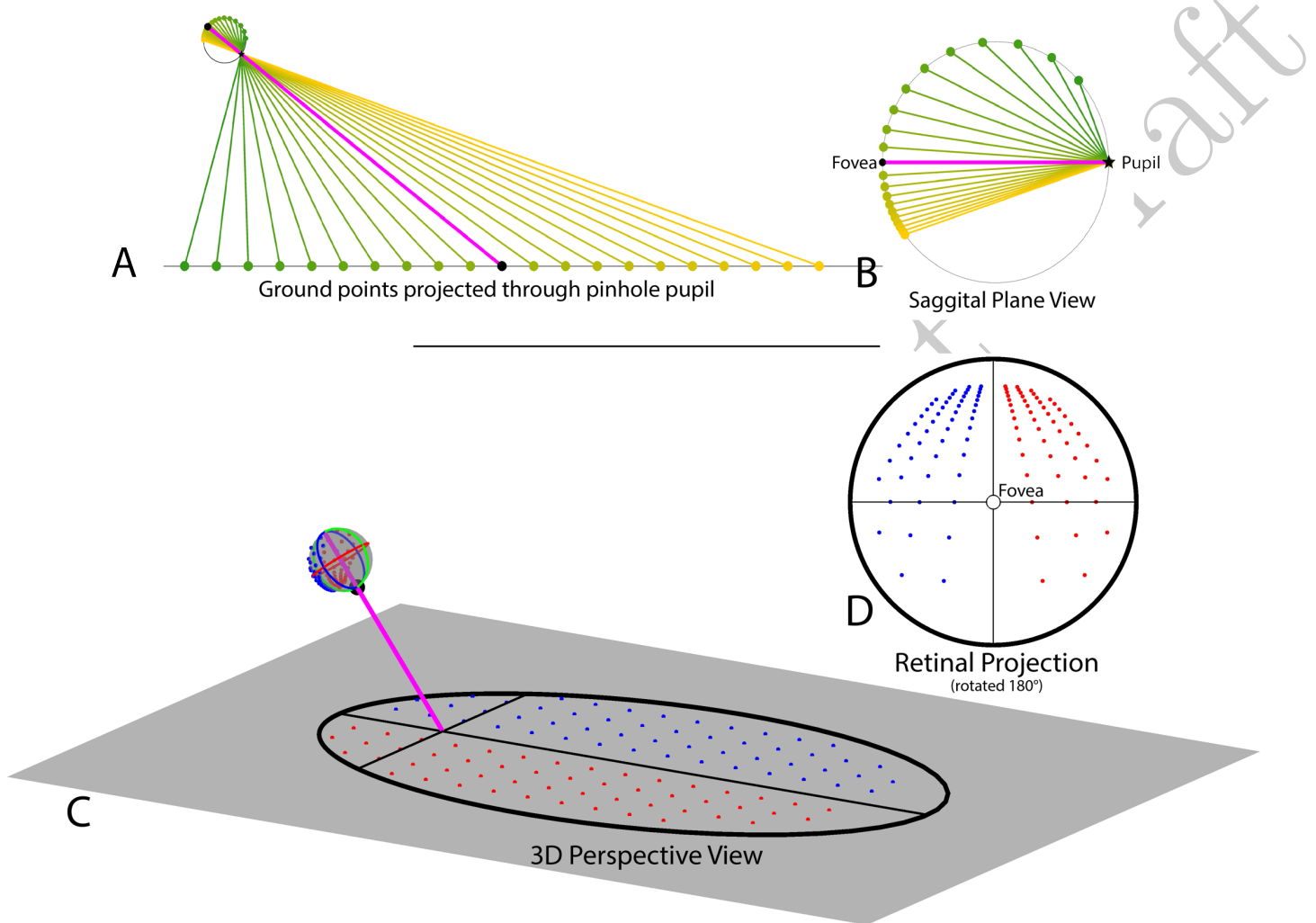


Figure 4. Spherical Pinhole Camera Model of the Eye. The spherical pinhole camera model of the eye used to estimate retinal optic flow experienced during natural locomotion. A, B show a sagittal plane slice of the 3D eye model. A shows the eye fixating on a point on the ground (pink line shows gaze vector, black circle shows fixation point) as points in the upper (orange) and lower (green) visual fields project on the back of the eye after passing through a pinhole pupil. B shows a closer view of the sagittal slice of the eye model. C, D show the full 3D spherical pinhole eye model. C shows the 3D eye fixating a point on the ground (black crosshairs), with field of view (60 degree radius) represented by the black outline. Note that the circular field of view of the eye is elongated due to its projection onto the ground plane. Red and blue dots represent points in the right and left visual field, respectively. D shows the retinal projection of the ground points from C on the spherical eye model. Ground dot location in retinal projection is defined in polar coordinates (ϑ, ρ) relative to the fovea at $(0,0)$, with ϑ defined by the angle between that dot's position on the spherical eye and the 'equator' on the transverse plane of the eye (blue circle) and ρ defined as the great-circle (orthodromic) distance between that dot and the fovea of the spherical eye. The retinal projection has been rotated by 180 degrees so that the upper visual field is at the top of the image.

6). This shows that the curl of retinal flow around the fovea provides a metric for the walker's trajectory relative to their current point of fixation.

Thus, the magnitude of rotation around the point of fixation provides a quantitative cue for the walker's current trajectory relative to the point of fixation. Specifically, there will be zero net curl around the fovea when the walker is fixating a point that is aligned with their current trajectory, and positive/negative curl values for fixation to the left/right of the current trajectory, with the magnitude of the curl signal increasing proportional to the eccentricity of the fixation point (Video 8). This cue could be used to help the walker move the body in a particular direction relative to the current fixation location on the ground. Maintaining fixation on a specific location and turning until there is zero curl around the fovea would be an effective way for a walker to orient the body towards a specific location such as a desirable foothold in the upcoming terrain, correct for potential postural errors, or simply to maintain a straight heading by nulling the horizontal trajectory changes associated with steps made with the right or left foot (Video 10). Similarly, walkers might learn to predict a certain pattern of retinal flow for a given bodily movement, and values outside this range could provide a signal for balance control (Reimann, Fettrow, Thompson, & Jeka, 2018; Roth et al., 2016)

3.1.2 The point of maximum divergence encodes the body's over-ground momentum vector in retinotopic coordinates

Fixating a point on a point on the ground while moving forward creates a pattern of expansion centered around the point of fixation. The local expansion at each point of a vector field can be quantified by calculating the *divergence* of the vector field. Divergence can be intuitively thought of as the rate that an array of drifting particles would vacate each point flow field. In contrast to optic flow on a fronto-parallel plane, the distance gradient results in variation in motion parallax of points on the ground plane across the upper to lower visual field. Therefore, divergence of the resulting flow field is determined by the velocity of the eye relative to the fixated point combined with the parallax gradient of points on the ground plane (Koenderink & van Doorn, 1976). In the context of locomotion, the divergence field during a ground plane fixation results in a hill-like gradient with a peak denoting the point of maximum retinal divergence that is contained within the ellipsoidal isoline that passes through the point of fixation (green circle in Figure 5). During straight-line movement towards the point of fixation the foveal iso-ellipsoid begins in the lower visual field before constricting to a point when the observer is one eye height away from their point of fixation (that is, when their gaze angle is 45 degrees) and then expanding into the upper visual field (Figure 5A-C, Video 4-6, Note that this feature of the divergence field is affected by upward and downward trajectories of the eye (Video 7).

Projecting the retinal divergence map onto the ground plane reveals that the ground projection of the eye's velocity vector always passes through the point of maximum retinal divergence. This feature of retinal flow means that a walker could, in principle, discern their own world-centered ground velocity directly from retinal flow. It is not necessary to convert retinal flow to a head-centered reference frame to have access to information about locomotor heading. Locomotor heading may be determined directly in retinotopic coordinates. Thus it should be possible to determine the body's world-centered velocity vector directly from patterns of motion on the retina and since velocity is a proxy for momentum, this would also define the body's momentum vector in retinotopic coordinates as a function of time through the

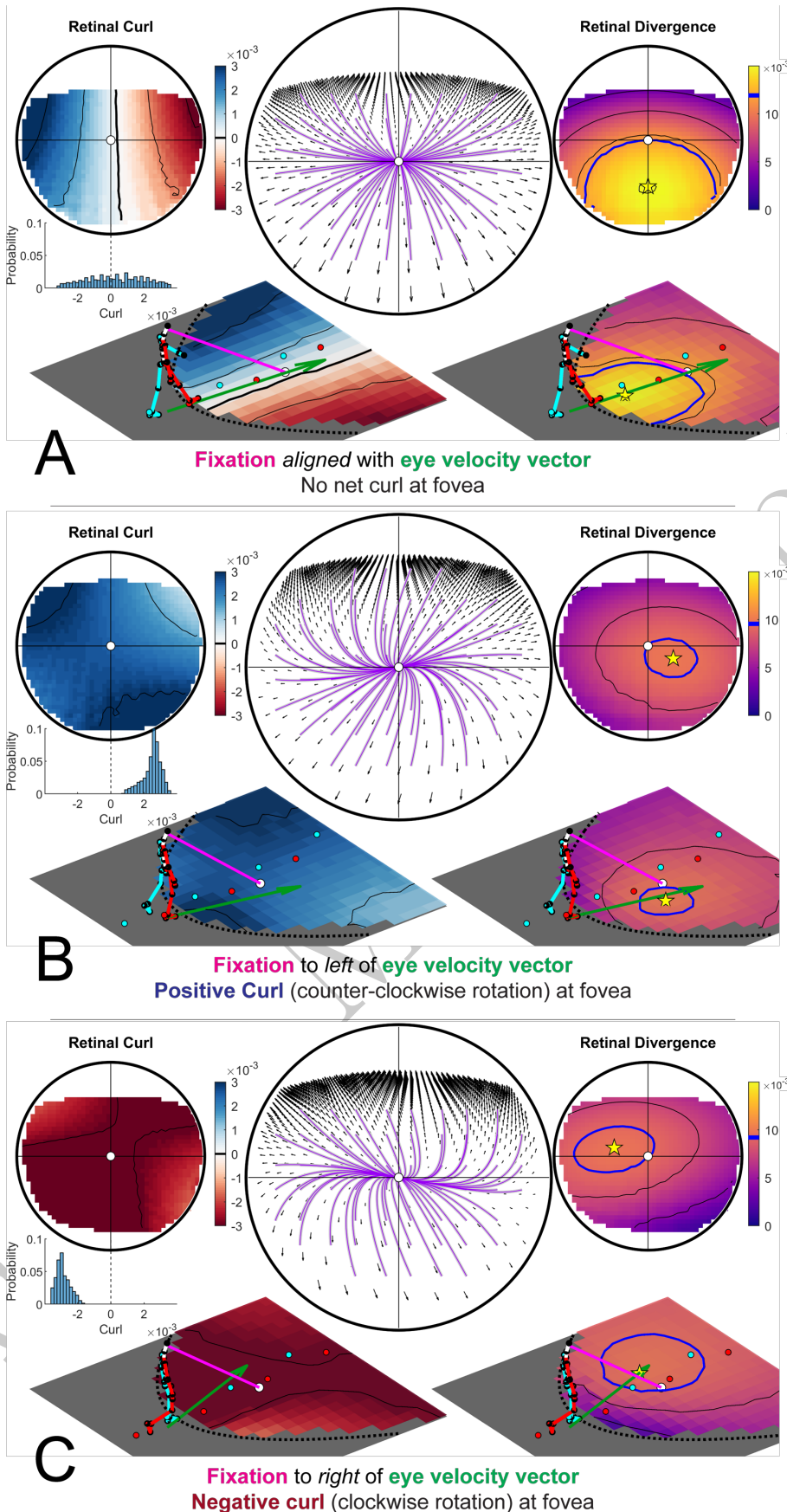


Figure 5. Retinal optic flow during natural locomotion. Retinal flow simulation based on integrated eye and full-body motion of an individual walking over real world terrain. Panels A-C are based on frames taken from Video2, which shows data derived from a subject walking in the Woodchips condition under the Ground Looking instructions. A shows a case where the fixation point (pink line) is aligned with ground projection of the eye's velocity vector (green arrow). Middle circular panel shows simulated optic flow based on fixation location and body movement. Left and right circular panels show the results of applying the curl and divergence operators to the retinal flow field in the middle panel. Left and right bottom panels show the projection of the curl (left) and divergence (right) onto a flat ground plane. The green arrow shows the walker's instantaneous velocity vector (scaled for visibility), which always passes through the maximum of the retinal divergence field, which always lies within the foveal isoline (blue circle). B and C show cases where the fixation point is to the left or right of the eye's velocity vector (respectively). Fixation to the left of the eye's velocity vector (B) results in a global counter-clockwise rotation of the retinal flow field and positive retinal curl at the fovea, while fixation to the right of the eye's velocity vector results in clockwise flow and negative curl at the fovea.

gait cycle. The body’s momentum vector is precisely the information a walker needs to make biomechanically informed decisions about where to place their feet so the ability of derive this information directly from retinal optic flow may be of critical importance for the control of locomotion. Therefore – assuming that the walker can determine the body-relative location of their fixation point (Crawford, Henriques, & Medendorp, 2011) – this analysis shows how patterns of stimulation on the retina might be directly related to the physical dynamics of bipedal locomotion (Matthis & Fajen, 2013, 2014; Matthis, Barton, & Fajen, 2015, 2017).

It should be noted that this simulation assumes a flat ground plane. In rocky or irregular terrain, local structure from motion will add complex local variations to the underlying retinal motion patterns described here, and it remains to be explored how these complexities might influence locomotion. It is likely that retinal motion cues from both eyes are combined to provide a robust estimate of both our movement through the 3d structure of the world, in what has been referred to as the “binoptic flow field” (Cormack, Czuba, Knöll, & Huk, 2017; Bonnen et al., 2020). Nonetheless, the monocular task-relevant features of retinal optic flow described here appear to be robust to complex, sinusoidal and circular simulate eye trajectories (Videos 9), locomotion over flat terrain (Video 10, showing a clip for the “Ground looking” condition on the Woodchips terrain), as well as the more circuitous routes taken in the rocky terrain (Videos 11, 12, and 13).

4 Discussion

We have demonstrated the ways that the optic flow patterns experienced during natural locomotion are shaped by the movement of the observer through their environments. By recording body motion during locomotion in natural terrain, we have demonstrated that head-centered optic flow is highly unstable. This is true whether the walker’s head (and eye) is directed towards a distant target or at the ground nearby to monitor foothold selection. In contrast, because gaze is stabilized by the VOR, the retinal optic flow has stable, reliable features that may be valuable for the control of locomotion. In particular, we found that a walker can determine whether they will pass to the left or right of their fixation point by observing the sign and magnitude of the curl of the flow field at the fovea. In addition, the divergence map of the retinal flow field provides a cue for the walker’s over-ground velocity/momentum vector, which may be an essential part of the visual identification of footholds during locomotion over complex terrain. These findings casts doubt on the assumption that accurate perception of heading direction requires correction for the effects of eccentric gaze, involving decomposition of the flow field into translational and rotational components, as has long been assumed (Li & Warren, 2004; Royden et al., 1994; Warren & Hannon, 1990; Yu, Hou, Spillmann, & Gu, 2017; Manning & Britten, 2019; Sunkara, DeAngelis, & Angelaki, 2016; Britten, 2008). The present analysis of retinal flow patterns during the gait cycle suggests an alternative interpretation of the way flow is used for both perception of heading and the control of locomotion. This is consistent with the suggestion of Wann and Land (2000) who argued that it was not necessary to correct for the effects of eccentric gaze. Glennerster et al. (2001) also argued that fixation might simplify rather than complicate the interpretation of flow.

Research on optic flow tends to implicitly assume that locomotion is well approximated by constant velocity motion along a straight (or sometime curved) path. This assumption is implicit in the choice of constant velocity stimuli in almost all

experimental paradigms. In addition to constant velocity, most experiments have used a stationary observer making judgments of simulated direction on a computer monitor (Li & Cheng, 2013; Li & Niehorster, 2014; R. Chen et al., 2017). These stimuli provide a strong sense of illusory motion (orvection) and subjects make highly accurate judgements about their simulated heading in these flow fields. These results indicate that humans are highly sensitive to full field optic flow, but this does not mean that the simulated self-motion stimuli are a good match for the stimuli experienced during natural locomotion. Nor does it necessarily mean that subjects use this information to control direction of the body when heading towards a distant goal. As we have shown here, human walking generates a complex, phasic pattern of acceleration that derives from the basic biomechanics of bipedal locomotion. In principle, knowing the motion of the head during locomotion makes it possible to infer the FoE, although the rapidity of its movement would be challenging given the time course of neural computations, and the instability may render it effectively unusable as a control variable. The issue of head movements has been raised previously (e.g. discussions of optic flow 'jitter' in van den Berg and Beintema (2000); Nakamura et al. (2016); Palmisano et al. (2000)), but in the absence of direct measurements of flow during locomotion the magnitude of the effect of gait has not been obvious. Thus it has been implicitly assumed that the overall structure of optic flow during locomotion would be dominated by the effects of forward motion (that is, that the FoE would be a good cue for heading). The present work directly measures head-centered flow during locomotion, and finds that instability in the head-centered flow fields are large enough that classical FoE-based theories about the use optic flow to control locomotion could not be realized on the basis of the visual stimulus experienced during natural locomotion.

4.1 The use of optic flow during natural locomotion

Despite the differences between the naturally occurring flow patterns described here and the optic flow stimuli typically used in psychophysical and electrophysiological experiments, the existing body of literature on optic flow strongly suggests that humans are adept at using flow patterns to determine their heading in simulated flow fields. However, since the present data show that the naturally occurring optic flow stimulus bears little resemblance to these simulated flow fields, how, then, might the flow information be used during natural locomotion?

The majority of research on the role of optic flow focuses on how humans steer to a distant target, but the many of the primary challenges of human walking operate on much shorter timescales. For all its practical advantages, striding bipedalism is inherently unstable – successful locomotion requires a walker to constantly regulate of muscle forces to support the mass of the body above the ground (McGowan, Neptune, Clark, & Kautz, 2010; Zajac, Neptune, & Kautz, 2002). In complex, rough terrain, these supporting muscle forces critically depends on the careful placement of the feet onto stable areas of terrain that are capable of supporting the walker's body while redirecting the momentum of their center of mass towards future footholds (Matthis et al., 2017, 2018). Failure to place the foot in a stable location or failure to properly support the body within a step may result in catastrophic injury. Given that walkers place their foot in a new location roughly twice per second, it is reasonable to assume that the underlying visual-motor control processes for foot placement and balance are fast, reliable, and efficient.

Indeed, optic flow has been shown to exert an important regulatory influence on the short-term components of gait. Expansion and contraction of optic flow patterns

entrain the gait of subjects walking on treadmills, with the steps phase-locked to timing of expansion and contraction in the flow patterns (Bardy, Warren, & Kay, 1996, 1999; Warren, Kay, & Yilmaz, 1996). Additional research has shown that optic flow can speed up adaptation to an asymmetric split-belt treadmill (Finley, Statton, & Bastian, 2014). Other evidence indicates that the FoE had a strong influence on posture but not on heading (Schubert, Bohner, Berger, v. Sprundel, & Duysens, 2003).

Salinas, Wilken, and Dingwell (2017) and Thompson and Franz (2017) have also demonstrated regulation of stepping by optic flow, and Reimann et al. (2018) has shown that optic flow perturbations produce a short-latency response in the ankle musculature. O'Connor and colleagues have shown that optic flow perturbations have a stronger effect when they are in a biomechanically unstable direction during standing and walking (O'Connor & Kuo, 2009), and that treadmill walkers will rapidly alter their walking speed to match altered optic flow before slowly adjusting back to their biomechanically preferred speed (O'Connor & Donelan, 2012). Taken together this body of research indicates a robust and sophisticated relationship between optic flow and the regulation of the short timescale biomechanical aspects of locomotion. The retinal optic flow cues described in this paper suggest much better candidates for the control variables that support this kind of locomotor control than head-centered FoE.

4.2 Optic flow, visual direction, and the control of locomotor heading

The view of the role of retinal flow in control of locomotion presented in this paper may resolve a long-standing debate about whether walkers control heading towards a goal on the basis of head-centered optic flow (and the focus of expansion, FoE) or visual direction. The present analysis reveals that the classically considered head-centered FoE during natural locomotion is poorly suited for this purpose. An alternative to flow for control of heading is visual direction – Rushton et al. (1998) proposed that the perceived location of a target with respect to the body is used to guide locomotion, rendering optic flow unnecessary. However, in a compelling demonstration, Warren et al. (2001) pitted visual direction against the focus of expansion in a virtual environment, where walkers generate the flow patterns typical with natural locomotion as we have measured here. They found that although visual direction was used to control walking paths when environments lacked visual structure (and thereby lacked a salient optic flow signal), optic flow had an increasing effect on paths as environments became more structured. The authors interpreted this result to mean that walkers use a combination of visual direction and optic flow (and the FoE) to steer to a goal when the visual environment contains sufficient visual structure. This is puzzling in the context of our findings, since the Warren et al. (2001) experiment used a fully ambulatory virtual environment, so the head-centered FoE experienced those subjects would have had the same instabilities described here. How then can we reconcile these results?

In the Warren et al. (2001) experiment, the FoE and visual direction were put in conflict using a virtual prism manipulation that displaces the visual direction of the goal but not the FoE. However, in light of the present study, it seems that this prism manipulation would also induce a change in the retinal curl subjects experienced during forward locomotion. To see why, imagine a walker (without prisms) moving forward while fixating a point that is directly on their travel path. As described above, this walker would experience no net curl at their point of fixation. Now imagine the same situation for a walker wearing prism glasses that shift their visual environment

10 degrees to the right – In that case, an individual walking forward while fixating a point that is directly on their travel path would experience retinal flow consistent with fixating a point that was 10 degrees to their right. Therefore, the walker would experience a retinal flow field with counter-clockwise rotation (negative curl) as in Figure 5C and Video 6. If walkers use this retinal flow cue to control their heading, this effect might drive them to turn their body in the opposite direction within a step, in order to null this illusory retinal rotation/curl, resulting in a straighter path towards the goal. Put another way, retinal curl provides a moment-to-moment error signal that the walkers could use to actively correct for the effects of the prism. This hypothetical locomotor effect would be most pronounced in environments with salient optic flow, which could explain why the authors found that subjects walked in straighter lines in visually structured environments. In this interpretation, the walker’s act of directing gaze towards their goal provides an egocentric heading cue to help them steer towards their target while retinal optic flow provides an error signal that may be used to control their locomotion and balance on a shorter timescale.

The present conception provides a theoretical framework for the visual control of locomotion that unifies research on longer-timescale control of steering towards a goal (Fajen, 2003) with the shorter-timescales associated with control of the mechanical aspects of balance and trajectory within a step. This framework provides an avenue for connecting control-law based research on perception and action (Warren, 2006) with the current state of visual neuroscience. Perception/Action research provides sophisticated (but neurally ungrounded) explanations of rich behaviors, while visual neuroscience provides a detailed explanation of the neural underpinnings of bland psychophysical tasks. By providing a link between the world-centered reference frame of mechanics and movement to the retinotopic reference frame of the early visual cortex, the present work may facilitate the development of a more complete theory of the neural underpinnings of visually guided behavior in the natural world.

4.3 Cortical involvement in the perception of optic flow

One of the insights from the observations in this study is that the stimulus input to the visual system is critically dependent on both the movement of the body and the gaze sampling strategies, especially in the case of motion stimuli. Gaze patterns in turn depend on behavioral goals. In rough terrain gaze is mostly on footholds 2-3 steps ahead, whereas in regular terrain gaze is mostly directed to more distant locations (Matthis et al., 2018). This changes the pattern of flow on the retina as demonstrated. If humans learn the regularities in the flow patterns and use this information to modulate posture and control stepping, investigation of the neural analysis of optic flow ideally requires patterns of stimulation that faithfully reflect the patterns experienced during natural movement. A variety of regions in both monkey and human cortex respond to optic flow patterns and have been implicated in self motion perception, including MT, MST, VIP, CSv (Morrone et al., 2000; Wall & Smith, 2008; Yu et al., 2017; X. Chen et al., 2013; Sunkara, DeAngelis, & Angelaki, 2015; Sunkara et al., 2016) and activity in these areas appears to be linked to heading judgments. However, there is no clear consensus on the role of these regions in the control of locomotion. For example, in humans, early visual regions and MT respond about equally to motion patterns that are inconsistent with self-motion (for example, when the FoE is not at the fovea) as they do to consistent patterns. MST had intermediate properties (Wall & Smith, 2008). Similarly in monkeys selectivity for ego-motion compatible stimuli was never total in a range of areas including MST and VIP (Cottureau et al., 2017). Strong, Silson, Gouws, Morland, and McKeefry (2017) also conclude that

MST is not critical for perception of self-motion. Since a variety of different motion patterns have been used in these experiments, it may be necessary to simulate the consequences of self-motion with stimuli more closely matched to the natural patterns. Many neurons within MST respond vigorously to spiral patterns of motion, which is notable in light of the ubiquitous spiral patterns that appear in the present dataset (e.g. Video 3 and 12). Interestingly, although neurons in both MST and VIP signal heading, they do not strongly discriminate between the retinal patterns generated by simulated, as opposed to real, eye movements (Sunkara et al., 2015; Manning & Britten, 2019). This suggests that the information critical for heading is computed in a retinal reference frame (Sunkara et al., 2015; X. Chen, DeAngelis, & Angelaki, 2018). Similarly, Bremmer et al. (2017) used a decoding model to estimated heading from the MST of monkeys looking at flowfields and noted that their reliability dropped every time the monkeys made a saccade, indicative of a neural system meant to extract heading on a per-fixation basis. This result is consistent with the suggestion of the present paper, that heading can be computed directly from the retinal patterns, and does not require subtraction of the rotational component to recover head-centered direction. The use of retinal flow for the control of movement requires that a walker has a notion of the body-relative location of their current fixation (Crawford et al., 2011), which might explain the well-established connection between vestibular cues and optic flow parsing (MacNeilage, Zhang, DeAngelis, & Angelaki, 2012).

5 Conclusion

Gibson's critical insight on optic flow was that an agent's movement through their environment imparts a structure to the available visual information, and that that structure can be exploited for the control of action (Gibson, 1950). In the intervening years, a large and fruitful body of research built upon this insight. However, the way optic flow is used by the visual system is difficult to intuit without direct measurement of the flow patterns that humans generate during natural behavior. Advances in imaging technology and computational image analysis, together with eye and body tracking in natural environments, have made it possible to measure and quantify these complex aspects of the visual input. Examination of the retinal flow patterns in the context of fixating and locomoting subjects suggests a change in emphasis and reinterpretation of the perceptual role of optic flow, emphasizing its role in balance and step control rather than in control of steering toward a goal. While many methods exist to compute instantaneous heading from the flow field, a consideration of these patterns relative to the gaze point through the gait cycle provides a context for the way the retinal flow information is used. More realistic analysis of the structure of the visual motion that we experience during natural locomotion, may allow a better understanding of the neural underpinnings of locomotor behavior in the natural world.

6 Acknowledgements

This work was supported by NIH 1T32-EY021462, R01-EY05729, and K99/R00-EY028229. Special thanks to John Cormack for his advice regarding the development of the streamline method for tracking the focus of expansion.

7 Methods and Materials

557

7.1 Experimental Subjects

558

Three human subjects participated in this experiment (1 female, 2 male; mean age: 28.7 +/-5 years, mean height: 1.79 +/- .14 m, mean weight: 78.3 +/- 18.8 kg, mean leg length: .96 +/- .68 m). One of the subjects was the first author of this manuscript. Subjects signed informed consent prior to participating in the experiment and all activities were approved by the Institutional Review Board at the University of Texas at Austin.

559

560

561

562

563

564

7.2 Equipment

565

Subjects' gaze was tracked using a Pupil Labs mobile eye tracker (Pupil Labs, Berlin, Germany). Each eye was recorded at 120Hz with 640x480 resolution (the eye cameras), while an outward facing camera mounted 3cm above the right eye (the world camera) recorded at 30Hz with 1920x1080 resolution and a 100degree diagonal field of view. Subjects' eyes were shaded using roll-up optometrist sunshades that covered the eyes and eye cameras but left the world camera uncovered. This method of shading the infrared eye cameras from sunlight was less robust than the full IR blocking face shield used in (Matthis et al., 2018), but was necessary to prevent the computational video analysis algorithms (described below) from being affected by reflections on the inside of the mask. For this reason, data collection was conducted during a time of day when the walking path was mostly shaded from direct sunlight. Kinematics were recorded using the Motion Shadow full body motion capture system using inertial measurement units recording at 100Hz. Raw data were initially recorded on a backpack-mounted laptop worn by the subject and later post-processed using custom code written for Matlab (MathWorks, Natick, MA, USA).

566

567

568

569

570

571

572

573

574

575

576

577

578

579

580

7.3 Data and code availability

581

In the fullness of time, all raw data will be posted in an online repository along with the Matlab code necessary to recreate each of the figures and videos in this manuscript.

582

583

584

7.4 Experimental Task

585

Subjects walked along two separate paths in the greenbelt of Austin TX, USA– A flat, tree-lined path consisting of mulched woodchips in the Shoal Creek trail in Pease District Park (the “woodchips path”) and a rough, rocky creekbed consisting mostly of large boulders (the “Rocky path”). The woodchips path was selected because it was flat enough that foot placement did not require visual guidance, but was visually textured enough for the optical flow detection algorithms to detect visual motion (in contrast to something like a concrete sidewalk). The rocky path was the same path used in the Rough Terrain condition of Matthis et al. (2018).

586

587

588

589

590

591

592

593

Subjects walked from start to the end of the Woodchips path while following one of three sets of instructions – Free walking, Ground looking, and Distant Fixation. In the Free Walking condition, subjects were instructed to simply walk from the start to the end location without any explicit instructions for what to do with their eyes.

594

595

596

597

In the Ground Looking condition, subjects were asked to walk while looking at the ground at an approximately fixed distance ahead. In the Distant Fixation condition, subjects were asked to walk while maintaining fixation on a self-selected distant object that was roughly at eye height (switching targets as necessary to maintain distant fixation). This condition was intended to most closely match the psychophysical tasks involved in previous research on optic flow during locomotion, i.e. fixation on a distant object while moving forward without head movement. Locomotion in the Rocky trail was challenging enough that subjects were not asked to complete a secondary task. They were simply asked to walk from the start to end position at a comfortable walking pace.

Subjects completed three out-and-back walks in the woodchips path, for a total of 6 trial/walks in that condition. There were two repetitions of each condition in the woodchips (one per walking direction). Subjects completed 4 out-and-back walks on the Rocky path, for total of 8 trial/walks. Because the woodchips path was significantly longer than the rocky path, a similar amount of data was collected in each condition.

7.5 VOR-based calibration and data postprocessing

We used a procedure analogous to the VOR-based calibration method developed in Matthis et al. (2018), with some alternations due to the change in eye tracker. The Pupil Labs tracker used in this study estimate gaze for each eye using 3D spherical eye models generated within the coordinate frame of each eye camera. Using the procedure described below, the gaze estimates for each eye were rotated to align with the reference frame of the full-body kinematic estimates from the IMU-based motion capture system.

The calibration procedure was completed at the start of data recording for each terrain condition for later processing. Subjects stood on a calibration mat that had marks for the subjects' feet, a high visibility marker located 1.4 m ahead of the vertical projection of the midpoint of the ankle joint, and a 0.5 m piece of tape at the same distance. Following the experimenter's instruction, subjects maintained fixation on that point while slowly moving their heads up/down, left/right, and along the diagonals. In addition to help determine the subject's 3D gaze vector by relating eye and head movements, data from this portion of the record were used to calibrate the eye tracker (similar to the "head tick" method described in Evans, Jacobs, Tarduno, and Pelz (2012), except that our subjects moved their heads smoothly).

The post-processing procedure to determine the subjects' world-centered 3D gaze vector is described below. Note that because each eye was calibrated independently, so any alignment between the gaze vectors of the right and left eye is an indication that the calibration was completed accurately.

1. Align timestamps of Pupil eye tracker and Shadow IMU data. Because the eye tracker and the motion capture system were being recorded on the same backpack mounted laptop, the timestamps from the two systems were already synchronized. Aligning the two data streams was a relatively simple matter of ensuring that both systems calculated time relative to some external temporal reference (rather than some unknown internal reference, such as "computer boot time").
2. Resample data from eye tracker and IMU to ensure constant 120Hz framerate. Kinematic data from the Shadow system (recorded at 100Hz) were upsampled

to 120Hz to match the framerate of the eye cameras. Following this, the left eye, right eye, and kinematic data streams were resampled to synchronize the three data streams.

3. Estimate eye center coordinates relative to head position estimates from Shadow system. This location will serve as the center for the spherical eye model generated by the Pupil Labs eye tracker.
4. Situate 3D spherical eye model from Pupil tracker onto eye center estimate calculated in step 3. Because this eye model was generated in the reference frame of the relevant eye camera, gaze vector orientations will be arbitrary when placed in the world-centered reference frame of the kinematic data from the Shadow system. The next step will align these gaze vectors with the subjects' world-centered gaze.
5. Use data from VOR calibration task to rotate gaze data from Pupil tracker to align with the subjects' world-centered gaze using unconstrained optimization (MATLAB's `fminunc` function).
 - (a) Begin with a starting guess where the Euler angle rotation of the gaze data is $[0\ 0\ 0]$.
 - (b) Rotate all gaze data by this rotation, and then rotate each gaze vector by the subject's head orientation on the frame that it was recorded.
 - (c) Calculate intersections between each gaze vector and the ground plane. If a gaze vector does not intersect the ground plane, truncate it at 10 m.
 - (d) Calculate error of this camera alignment rotation, defined as the mean distance between the intersection point of each gaze vector and the calibration point that subjects were fixating (located 1.4 m ahead of the vertical projection of the subject's ankle joints).
 - (e) Use `fminunc` to minimize this error by optimizing the Euler angle rotation to apply to the gaze vectors prior to applying the rotation specified by the subject's head orientation. The correct orientation will cause subjects' head rotations to cancel their eye movements to maintain the gaze vector alignment with the calibration point (that is, the correct gaze alignment rotation will preserve VOR-based eye compensation for head rotation).
6. Once the correct gaze alignment rotation has been identified, apply it to all subsequent gaze data from this recording prior to rotating each gaze point according to the subject's head orientation on that data frame.

7.6 Video Analysis and optic flow estimation

We used the Matlab Camera Calibration toolbox to estimate the lens intrinsics of the head-mounted world camera of the Pupil tracker (3 radial distortion coefficients with skew correction). This method utilizes a checkerboard of known size to determine the distortion caused by the wide angle lens of the camera. This calibration effectively allows us to treat the images from the head mounted camera as if they were recorded by a linear pinhole camera. We then estimated the visual motion on each recorded frame of the head-mounted camera using the Deep Flow optical flow estimation algorithm (Weinzaepfel et al., 2013) in OpenCV (Bradski & Kaehler, 2011). DeepFlow is a dense optical flow estimation algorithm that provides a motion estimate at each pixel of each frame of the analyzed video. Despite its name, this method

does not rely on deep learning methods to detect optic flow. Internal testing found
that deep-learning based methods are prone to biases (likely due to their training
data), and so are not appropriate for use as a scientific research method.

7.6.1 Estimating retinal reference frame

In order to estimate the visual stimulus in a retinal reference frame, each recorded
frame from the undistorted world camera was projected onto a sphere and placed so
that that subjects' point of regard on that frame was aligned with 0,0 in the retinal
reference frame. To account for inaccuracy in this eye tracker, fixations were "ideal-
ized" by adjusting the placement of the image to null any residual motion detected at
that point of fixation. (Inspection of the videos revealed only minimal residual motion
during fixation.) In this way, the retinal reference frame videos provide an estimate
of the visual motion that was incident to the subjects' retina, assuming "perfect"
fixation and a spherical pinhole camera model of the eye.

7.7 Optic Flow simulation with a spherical pinhole camera model of the eye

We created a geometric simulation to provide a more nuanced picture of the way
that the movement of the body shapes the visual motion experienced during natural
locomotion. To estimate the flow experienced during various types of movements,
a simulated eye model was generated using the following procedure. Most of the
geometric calculations used in this model rely heavily on the Geom3D toolbox on
Mathworks.com (Legland, 2020)

1. Define the groundplane as an infinite, flat plane with zero height.
2. Define an evenly spaced grid of points on the ground plane, which will eventu-
ally be projected onto the back of the simulated retina.
3. Define the spherical eyeball as a sphere with a radius of 12 mm (the anatomi-
cal average radius of the human eye). In this model, one pole of the sphere is
defined as the 'pupil' and the opposite pole is defined as the 'fovea'. Place the
center of this eye model at the correct location in 3D space. This location is
either determined from the recorded motion capture data (as in Videos 10 and
13) or by determining a prescribed path for the eye to follow (as in Videos 4 - 9)
4. Rotate the eye model to face the fixation point on that frame. Orient the eye
so that there is a line passing through so that a line passing through fovea and
pupil will also pass through the fixation point on the ground. This rotation was
defined so as to minimize torsion about the optical axis.
5. Define the field of view of the eye by projecting a cone from the pupil determi-
ning the intersection points between this cone and the flat ground plane. For this
study, we defined the field of view cone to have a 60 degree radius..
6. Project all the groundpoints within the field of view through the pupil and onto
the back of the 3D spherical retina.
7. Resituate projected points onto a 2D polar plot where the vertical axis ($\pi/2$)
defines the anatomical superior of the eye, and the eccentricity is defined as the
"great circle" distance of the projected point from the 'fovea' of the spherical

eye. Keep track of these projected locations across successive frames, to allow
for calculation of optic flow on later steps.

8. Calculate flow per frame by determining the distance between the projection
of each point on successive frames. The flow on the first frame is defined to be
zero everywhere. If a particular point was not within the eye's field of view on
the previous frame, flow at that point is undefined on the first frame that point
became visible.
9. Use the scatteredInterpolant function in Matlab to define an evenly spaced
vector field across the retina that shares the structure of the projected-dot flow
field determined in the previous step. This step is necessary to be able to calcu-
late the Curl and Divergence of the vector field.
10. Calculate divergence and curl of this evenly spaced retinal velocity grid using
the divergence and curl functions in Matlab.
11. Spend two years fastidiously creating overcomplicated videos to highlight vari-
ous features of the resulting flowfields (optional)

7.7.1 Estimating the Focus of Expansion

To estimate the location of the focus of expansion on each frame, each frame
from world camera was first processed by the DeepFlow optical flow algorithm de-
scribed above. This method provides a motion estimate for each pixel of the video
frame, providing a 2 dimensional vector field with the same dimension as the original
video for each recorded frame. To track the Focus of Expansion (FoE) in each frame,
this vector field was first negated (all vectors were multiplied by -1), which effectively
transforms the FoE from a repeller node (vectors pointing away from the FoE) into
an attractor node (vectors pointing towards the FoE). Then, a grid of particles was
set to drift on this negated flow field using the streamlines2 function in Matlab. The
paths traced by these particles provide information about the underlying structure of
the optic flow on each frame, represented as white lines in Figures and Video. These
streamlines represent the line integrals of the optic flow vector field measured on each
frame.

The location of the FoE was determined by keeping track of the final fate of each
of the drifting particles and tagging the location where the majority ended up as the
pixel location of the FoE on that frame. On frames where fewer than 50% of parti-
cles could be found in a particular location on the video screen, it was determined
that the FoE was not in the field of view of the camera on that frame (this could be
verified visually by noting that the streamlines on those frames do not converge to a
single point). To calculate the velocity of the FoE on each frame, we calculated the
2D distance traveled by the FoE on successive frames, multiplied by that by the field
of the view of the camera (to convert to Degrees Visual Angle) and then divided by
the framerate (to convert to Degrees per second).

To ensure that this method was capable of detecting a stable FoE (that is, to
ensure that the high velocity of the FoE that we record was not just an artifact of
the detection method), we applied this analysis to the video from a DJI Phantom
4 quadcopter as it traveled along a straight horizontal and vertical flight path. The
camera of this quadcopter is stabilized by a 3-axis gimbal mount, which is essentially
a mechanical equivalent of the VOR-reflex. The resulting FoE is nicely stable, indicat-
ing that this method is capable of detecting a stable, low-velocity FoE in a video, if it
is present (Video 14).

References

779

- Bardy, B. G., Warren, W. H., & Kay, B. A. (1996, September). Motion parallax is used to control postural sway during walking. *Experimental Brain Research*, *111*(2), 271–282. doi: 10.1007/BF00227304 780
- Bardy, B. G., Warren, W. H., & Kay, B. A. (1999, October). The role of central and peripheral vision in postural control during walking. *Perception & Psychophysics*, *61*(7), 1356–1368. doi: 10.3758/bf03206186 781
- Bonnen, K., Czuba, T. B., Whritner, J. A., Kohn, A., Huk, A. C., & Cormack, L. K. (2020, January). Binocular viewing geometry shapes the neural representation of the dynamic three-dimensional environment. *Nature Neuroscience*, *23*(1), 113–121. Retrieved 2020-07-22, from <http://www.nature.com/articles/s41593-019-0544-7> doi: 10.1038/s41593-019-0544-7 782
- Bradski, G. R., & Kaehler, A. (2011). *Learning OpenCV: computer vision with the OpenCV library* (1. ed., [Nachdr.] ed.). Beijing: O'Reilly. (OCLC: 838472784) 783
- Bremmer, F., Churan, J., & Lappe, M. (2017, December). Heading representations in primates are compressed by saccades. *Nature Communications*, *8*(1), 920. Retrieved 2020-07-22, from <http://www.nature.com/articles/s41467-017-01021-5> doi: 10.1038/s41467-017-01021-5 784
- Britten, K. H. (2008, July). Mechanisms of Self-Motion Perception. *Annual Review of Neuroscience*, *31*(1), 389–410. Retrieved 2020-07-18, from <http://www.annualreviews.org/doi/10.1146/annurev.neuro.29.051605.112953> doi: 10.1146/annurev.neuro.29.051605.112953 785
- Chen, A., Gu, Y., Liu, S., DeAngelis, G. C., & Angelaki, D. E. (2016, March). Evidence for a Causal Contribution of Macaque Vestibular, But Not Intraparietal, Cortex to Heading Perception. *The Journal of Neuroscience*, *36*(13), 3789–3798. Retrieved 2020-07-18, from <http://www.jneurosci.org/lookup/doi/10.1523/JNEUROSCI.2485-15.2016> doi: 10.1523/JNEUROSCI.2485-15.2016 786
- Chen, R., Niehorster, D. C., & Li, L. (2017). Effect of travel speed on the visual control of steering toward a goal. *Journal of Experimental Psychology: Human Perception and Performance*, *44*(3), 452–467. Retrieved 2020-07-20, from <http://doi.apa.org/getdoi.cfm?doi=10.1037/xhp0000477> doi: 10.1037/xhp0000477 787
- Chen, X., DeAngelis, G. C., & Angelaki, D. E. (2013, November). Eye-Centered Representation of Optic Flow Tuning in the Ventral Intraparietal Area. *Journal of Neuroscience*, *33*(47), 18574–18582. Retrieved 2020-07-18, from <http://www.jneurosci.org/cgi/doi/10.1523/JNEUROSCI.2837-13.2013> doi: 10.1523/JNEUROSCI.2837-13.2013 788
- Chen, X., DeAngelis, G. C., & Angelaki, D. E. (2018, April). Flexible egocentric and allocentric representations of heading signals in parietal cortex. *Proceedings of the National Academy of Sciences*, *115*(14), E3305–E3312. Retrieved 2020-07-20, from <http://www.pnas.org/lookup/doi/10.1073/pnas.1715625115> doi: 10.1073/pnas.1715625115 789
- Cormack, L. K., Czuba, T. B., Knöll, J., & Huk, A. C. (2017, September). Binocular Mechanisms of 3D Motion Processing. *Annual Review of Vision Science*, *3*(1), 297–318. Retrieved 2020-07-18, from <http://www.annualreviews.org/doi/10.1146/annurev-vision-102016-061259> doi: 10.1146/annurev-vision-102016-061259 790
- Cottureau, B. R., Smith, A. T., Rima, S., Fize, D., Héjja-Brichard, Y., Renaud, L., ... Durand, J.-B. (2017, January). Processing of Egomotion-Consistent Optic Flow in the Rhesus Macaque Cortex. *Cerebral Cortex*, cercor:bhw412v1. Retrieved 2020-07-20, from <https://academic.oup.com/cercor/article-lookup/doi/10.1093/cercor/bhw412> doi: 10.1093/cercor/bhw412 791

- Crawford, J. D., Henriques, D. Y., & Medendorp, W. P. (2011, July). Three-Dimensional Transformations for Goal-Directed Action. *Annual Review of Neuroscience*, *34*(1), 309–331. Retrieved 2020-08-03, from <http://www.annualreviews.org/doi/10.1146/annurev-neuro-061010-113749> doi: 10.1146/annurev-neuro-061010-113749
- Dietrich, H., & Wuehr, M. (2019, June). Strategies for Gaze Stabilization Critically Depend on Locomotor Speed. *Neuroscience*, *408*, 418–429. Retrieved 2020-07-18, from <https://linkinghub.elsevier.com/retrieve/pii/S0306452219300454> doi: 10.1016/j.neuroscience.2019.01.025
- Donelan, M., Kram, R., & Kuo, A. D. (2001, October). Mechanical and metabolic determinants of the preferred step width in human walking. *Proceedings of the Royal Society of London. Series B: Biological Sciences*, *268*(1480), 1985–1992. Retrieved 2020-07-18, from <https://royalsocietypublishing.org/doi/10.1098/rspb.2001.1761> doi: 10.1098/rspb.2001.1761
- Duffy, C. J., & Wurtz, R. H. (1991, June). Sensitivity of MST neurons to optic flow stimuli. I. A continuum of response selectivity to large-field stimuli. *Journal of Neurophysiology*, *65*(6), 1329–1345. Retrieved 2020-07-18, from <https://www.physiology.org/doi/10.1152/jn.1991.65.6.1329> doi: 10.1152/jn.1991.65.6.1329
- Evans, K. M., Jacobs, R. A., Tarduno, J. A., & Pelz, J. B. (2012). Collecting and Analyzing Eye-tracking Data in Outdoor Environments. *R. A.*, 19.
- Fajen, B. R. (2003). A Dynamical Model of Visually-Guided Steering, Obstacle Avoidance, and Route Selection. *International Journal of Computer Vision*, *54*(1/2), 13–34. Retrieved 2020-08-03, from <http://link.springer.com/10.1023/A:1023701300169> doi: 10.1023/A:1023701300169
- Finley, J. M., Statton, M. A., & Bastian, A. J. (2014, March). A novel optic flow pattern speeds split-belt locomotor adaptation. *Journal of Neurophysiology*, *111*(5), 969–976. Retrieved 2020-07-18, from <https://www.physiology.org/doi/10.1152/jn.00513.2013> doi: 10.1152/jn.00513.2013
- Gibson, J. J. (1950). *The perception of the visual world*. Westport, Conn: Greenwood Press.
- Gibson, J. J. (1979). *The ecological approach to visual perception*. New York, London: Psychology Press. (OCLC: 962481298)
- Glennerster, A., Hansard, M. E., & Fitzgibbon, A. W. (2001, March). Fixation could simplify, not complicate, the interpretation of retinal flow. *Vision Research*, *41*(6), 815–834. Retrieved 2020-07-18, from <https://linkinghub.elsevier.com/retrieve/pii/S004269890000300X> doi: 10.1016/S0042-6989(00)00300-X
- Kavanagh, J. J., & Menz, H. B. (2008, July). Accelerometry: A technique for quantifying movement patterns during walking. *Gait & Posture*, *28*(1), 1–15. Retrieved 2020-07-20, from <https://linkinghub.elsevier.com/retrieve/pii/S0966636207002706> doi: 10.1016/j.gaitpost.2007.10.010
- Koenderink, J. J. (1986, January). Optic flow. *Vision Research*, *26*(1), 161–179. Retrieved 2020-07-18, from <https://linkinghub.elsevier.com/retrieve/pii/0042698986900787> doi: 10.1016/0042-6989(86)90078-7
- Koenderink, J. J., & van Doorn, A. J. (1976, July). Local structure of movement parallax of the plane. *Journal of the Optical Society of America*, *66*(7), 717. Retrieved 2020-07-18, from <https://www.osapublishing.org/abstract.cfm?URI=josa-66-7-717> doi: 10.1364/JOSA.66.000717
- Koenderink, J. J., & van Doorn, A. J. (1984). Optical Monitoring of Ego-Motion for Movement with Respect to a Plane Surface. In D. Varjú & H.-U. Schnitzler (Eds.), *Localization and Orientation in Biology and Engineering* (pp. 163–166).

- Berlin, Heidelberg: Springer Berlin Heidelberg. Retrieved 2020-07-20, from http://link.springer.com/10.1007/978-3-642-69308-3_34 (Series Title: Proceedings in Life Sciences) doi: 10.1007/978-3-642-69308-3_34
- Kuo, A. D. (2007, August). The six determinants of gait and the inverted pendulum analogy: A dynamic walking perspective. *Human Movement Science*, 26(4), 617–656. Retrieved 2020-07-18, from <https://linkinghub.elsevier.com/retrieve/pii/S0167945707000309> doi: 10.1016/j.humov.2007.04.003
- Land, M. F. (2018). The Evolution of Gaze Shifting Eye Movements. In T. Hodgson (Ed.), *Processes of Visuospatial Attention and Working Memory* (Vol. 41, pp. 3–11). Cham: Springer International Publishing. Retrieved 2020-07-18, from http://link.springer.com/10.1007/7854_2018_60 (Series Title: Current Topics in Behavioral Neurosciences) doi: 10.1007/7854_2018_60
- Lappe, M., Bremmer, F., & van den Berg, A. (1999, September). Perception of self-motion from visual flow. *Trends in Cognitive Sciences*, 3(9), 329–336. Retrieved 2020-07-18, from <https://linkinghub.elsevier.com/retrieve/pii/S1364661399013649> doi: 10.1016/S1364-6613(99)01364-9
- Lappi, O. (2016, October). Eye movements in the wild: Oculomotor control, gaze behavior & frames of reference. *Neuroscience & Biobehavioral Reviews*, 69, 49–68. Retrieved 2020-07-18, from <https://linkinghub.elsevier.com/retrieve/pii/S0149763415301317> doi: 10.1016/j.neubiorev.2016.06.006
- Legland, D. (2020). *geom3d*. Matlab File Exchange. Retrieved from <https://www.mathworks.com/matlabcentral/fileexchange/24484-geom3d>
- Li, L., & Cheng, J. C. (2013, April). Visual strategies for the control of steering toward a goal. *Displays*, 34(2), 97–104. Retrieved 2020-07-20, from <https://linkinghub.elsevier.com/retrieve/pii/S0141938212000819> doi: 10.1016/j.displa.2012.10.005
- Li, L., & Niehorster, D. C. (2014, August). Influence of optic flow on the control of heading and target egocentric direction during steering toward a goal. *Journal of Neurophysiology*, 112(4), 766–777. Retrieved 2020-07-20, from <https://www.physiology.org/doi/10.1152/jn.00697.2013> doi: 10.1152/jn.00697.2013
- Li, L., & Warren, W. H. (2004, July). Path perception during rotation: influence of instructions, depth range, and dot density. *Vision Research*, 44(16), 1879–1889. Retrieved 2020-07-18, from <https://linkinghub.elsevier.com/retrieve/pii/S0042698904001087> doi: 10.1016/j.visres.2004.03.008
- Longuet-Higgins, H. C., & Prazdny, K. (1980). The interpretation of a moving retinal image. *Proceedings of the Royal Society B: Biological Sciences*, 208, 13. doi: <https://doi.org/10.1098/rspb.1980.0057>
- MacNeilage, P. R., Zhang, Z., DeAngelis, G. C., & Angelaki, D. E. (2012, July). Vestibular Facilitation of Optic Flow Parsing. *PLoS ONE*, 7(7), e40264. Retrieved 2020-08-03, from <https://dx.plos.org/10.1371/journal.pone.0040264> doi: 10.1371/journal.pone.0040264
- Manning, T. S., & Britten, K. H. (2019, October). Retinal Stabilization Reveals Limited Influence of Extraretinal Signals on Heading Tuning in the Medial Superior Temporal Area. *The Journal of Neuroscience*, 39(41), 8064–8078. Retrieved 2020-07-20, from <http://www.jneurosci.org/lookup/doi/10.1523/JNEUROSCI.0388-19.2019> doi: 10.1523/JNEUROSCI.0388-19.2019
- Matthis, J. S., Barton, S. L., & Fajen, B. R. (2015, March). The biomechanics of walking shape the use of visual information during locomotion over complex terrain. *Journal of Vision*, 15(3), 10. Retrieved 2020-07-22, from <http://jov.arvojournals.org/article.aspx?doi=10.1167/15.3.10> doi: 10.1167/15.3.10
- Matthis, J. S., Barton, S. L., & Fajen, B. R. (2017, August). The critical phase

- for visual control of human walking over complex terrain. *Proceedings of the National Academy of Sciences*, 114(32), E6720–E6729. Retrieved 2020-07-18, from <http://www.pnas.org/lookup/doi/10.1073/pnas.1611699114> doi: 10.1073/pnas.1611699114
- Matthis, J. S., & Fajen, B. R. (2013, July). Humans exploit the biomechanics of bipedal gait during visually guided walking over complex terrain. *Proceedings of the Royal Society B: Biological Sciences*, 280(1762), 20130700. Retrieved 2020-07-22, from <https://royalsocietypublishing.org/doi/10.1098/rspb.2013.0700> doi: 10.1098/rspb.2013.0700
- Matthis, J. S., & Fajen, B. R. (2014, February). Visual control of foot placement when walking over complex terrain. *Journal of Experimental Psychology: Human Perception and Performance*, 40(1), 106–115. Retrieved 2020-07-22, from <http://doi.apa.org/getdoi.cfm?doi=10.1037/a0033101> doi: 10.1037/a0033101
- Matthis, J. S., Yates, J. L., & Hayhoe, M. M. (2018, April). Gaze and the Control of Foot Placement When Walking in Natural Terrain. *Current Biology*, 28(8), 1224–1233.e5. Retrieved 2020-07-18, from <https://linkinghub.elsevier.com/retrieve/pii/S0960982218303099> doi: 10.1016/j.cub.2018.03.008
- McGowan, C. P., Neptune, R. R., Clark, D. J., & Kautz, S. A. (2010, February). Modular control of human walking: Adaptations to altered mechanical demands. *Journal of Biomechanics*, 43(3), 412–419. Retrieved 2020-07-18, from <https://linkinghub.elsevier.com/retrieve/pii/S002192900900582X> doi: 10.1016/j.jbiomech.2009.10.009
- Menz, H. B., Lord, S. R., & Fitzpatrick, R. C. (2003, August). Acceleration patterns of the head and pelvis when walking on level and irregular surfaces. *Gait & Posture*, 18(1), 35–46. Retrieved 2020-07-20, from <https://linkinghub.elsevier.com/retrieve/pii/S0966636202001595> doi: 10.1016/S0966-6362(02)00159-5
- Mochon, S., & McMahon, T. A. (1980, January). Ballistic walking. *Journal of Biomechanics*, 13(1), 49–57. Retrieved 2020-07-20, from <https://linkinghub.elsevier.com/retrieve/pii/002192908090007X> doi: 10.1016/0021-9290(80)90007-X
- Morrone, M. C., Tosetti, M., Montanaro, D., Fiorentini, A., Cioni, G., & Burr, D. C. (2000, December). A cortical area that responds specifically to optic flow, revealed by fMRI. *Nature Neuroscience*, 3(12), 1322–1328. Retrieved 2020-07-20, from <http://www.nature.com/articles/nn1200.1322> doi: 10.1038/81860
- Nakamura, S., Palmisano, S., & Kim, J. (2016, July). Relative Visual Oscillation Can Facilitate Visually Induced Self-Motion Perception. *i-Perception*, 7(4), 204166951666190. Retrieved 2020-07-20, from <http://journals.sagepub.com/doi/full/10.1177/2041669516661903> doi: 10.1177/2041669516661903
- O'Connor, S. M., & Donelan, J. M. (2012, May). Fast visual prediction and slow optimization of preferred walking speed. *Journal of Neurophysiology*, 107(9), 2549–2559. Retrieved 2020-07-18, from <https://www.physiology.org/doi/10.1152/jn.00866.2011> doi: 10.1152/jn.00866.2011
- O'Connor, S. M., & Kuo, A. D. (2009, September). Direction-Dependent Control of Balance During Walking and Standing. *Journal of Neurophysiology*, 102(3), 1411–1419. Retrieved 2020-07-18, from <https://www.physiology.org/doi/10.1152/jn.00131.2009> doi: 10.1152/jn.00131.2009
- Palmisano, S., Gillam, B. J., & Blackburn, S. G. (2000, January). Global-Perspective Jitter Improves Vection in Central Vision. *Perception*, 29(1), 57–67. Retrieved 2020-07-20, from <http://journals.sagepub.com/doi/10.1068/p2990> doi: 10.1068/p2990
- Paolini, M., Distler, C., Bremmer, F., Lappe, M., & Hoffmann, K.-P. (2000, August). Responses to Continuously Changing Optic Flow in Area MST. *Journal of*

- Neurophysiology*, 84(2), 730–743. Retrieved 2020-07-18, from <https://www.physiology.org/doi/10.1152/jn.2000.84.2.730> doi: 10.1152/jn.2000.84.2.730
- Patla, A., & Vickers, J. (2003, January). How far ahead do we look when required to step on specific locations in the travel path during locomotion? *Experimental Brain Research*, 148(1), 133–138. Retrieved 2020-07-18, from <http://link.springer.com/10.1007/s00221-002-1246-y> doi: 10.1007/s00221-002-1246-y
- Reimann, H., Fettrow, T., Thompson, E. D., & Jeka, J. J. (2018, September). Neural Control of Balance During Walking. *Frontiers in Physiology*, 9, 1271. Retrieved 2020-07-18, from <https://www.frontiersin.org/article/10.3389/fphys.2018.01271/full> doi: 10.3389/fphys.2018.01271
- Rogers, B. J., & Dalton, C. (1999). The role of (i) perceived direction and (ii) optic flow in the control of locomotion and for estimating the point of impact. In *INVESTIGATIVE OPHTHALMOLOGY & VISUAL SCIENCE* (Vol. 40, pp. S764–S764). (Number: 4 tex.organization: ASSOC RESEARCH VISION OPHTHALMOLOGY INC 9650 ROCKVILLE PIKE, BETHESDA, MD ...)
- Roth, M. M., Dahmen, J. C., Muir, D. R., Imhof, F., Martini, F. J., & Hofer, S. B. (2016, February). Thalamic nuclei convey diverse contextual information to layer 1 of visual cortex. *Nature Neuroscience*, 19(2), 299–307. Retrieved 2020-07-18, from <http://www.nature.com/articles/nn.4197> doi: 10.1038/nn.4197
- Royden, C. S., Banks, M. S., & Crowell, J. A. (1992, December). The perception of heading during eye movements. *Nature*, 360(6404), 583–585. Retrieved 2020-07-18, from <http://www.nature.com/articles/360583a0> doi: 10.1038/360583a0
- Royden, C. S., Crowell, J. A., & Banks, M. S. (1994, December). Estimating heading during eye movements. *Vision Research*, 34(23), 3197–3214. Retrieved 2020-07-18, from <https://linkinghub.elsevier.com/retrieve/pii/0042698994900841> doi: 10.1016/0042-6989(94)90084-1
- Rushton, S. K., Harris, J. M., Lloyd, M. R., & Wann, J. P. (1998, October). Guidance of locomotion on foot uses perceived target location rather than optic flow. *Current Biology*, 8(21), 1191–1194. Retrieved 2020-07-20, from <https://linkinghub.elsevier.com/retrieve/pii/S0960982207004927> doi: 10.1016/S0960-9822(07)00492-7
- Salinas, M. M., Wilken, J. M., & Dingwell, J. B. (2017, September). How humans use visual optic flow to regulate stepping during walking. *Gait and Posture*, 57, 15–20. Retrieved 2020-07-20, from <https://pennstate.pure.elsevier.com/en/publications/how-humans-use-visual-optic-flow-to-regulate-stepping-during-walk> (Publisher: Elsevier) doi: 10.1016/j.gaitpost.2017.05.002
- Schubert, M., Bohner, C., Berger, W., v. Sprundel, M., & Duysens, J. E. J. (2003, May). The role of vision in maintaining heading direction: effects of changing gaze and optic flow on human gait. *Experimental Brain Research*, 150(2), 163–173. Retrieved 2020-07-20, from <https://doi.org/10.1007/s00221-003-1390-z> doi: 10.1007/s00221-003-1390-z
- Strong, S. L., Silson, E. H., Gouws, A. D., Morland, A. B., & McKeefry, D. J. (2017, March). Differential processing of the direction and focus of expansion of optic flow stimuli in areas MST and V3A of the human visual cortex. *Journal of Neurophysiology*, 117(6), 2209–2217. Retrieved 2020-07-20, from <https://journals.physiology.org/doi/full/10.1152/jn.00031.2017> (Publisher: American Physiological Society) doi: 10.1152/jn.00031.2017
- Sunkara, A., DeAngelis, G. C., & Angelaki, D. E. (2015, February). Role of visual and non-visual cues in constructing a rotation-invariant representation of heading in parietal cortex. *eLife*, 4, e04693. Retrieved 2020-07-20, from <https://doi.org/10.7554/eLife.04693> (Publisher: eLife Sciences Publications, Ltd)

- doi: 10.7554/eLife.04693 1038
- Sunkara, A., DeAngelis, G. C., & Angelaki, D. E. (2016, May). Joint representation of 1039
translational and rotational components of optic flow in parietal cortex. *Proceed-* 1040
ings of the National Academy of Sciences, 113(18), 5077–5082. Retrieved 2020-07- 1041
20, from <http://www.pnas.org/lookup/doi/10.1073/pnas.1604818113> doi: 1042
10.1073/pnas.1604818113 1043
- Thompson, J. D., & Franz, J. R. (2017, August). Do Kinematic Metrics of Walking 1044
Balance Adapt to Perturbed Optical Flow? *Human movement science*, 54, 34–40. 1045
Retrieved 2020-07-20, from [https://www.ncbi.nlm.nih.gov/pmc/articles/](https://www.ncbi.nlm.nih.gov/pmc/articles/PMC6020025/) 1046
PMC6020025/ doi: 10.1016/j.humov.2017.03.004 1047
- van den Berg, A. V., & Beintema, J. A. (2000, June). The Mechanism of Interaction 1048
between Visual Flow and Eye Velocity Signals for Heading Perception. *Neuron*, 1049
26(3), 747–752. Retrieved 2020-07-22, from [https://linkinghub.elsevier](https://linkinghub.elsevier.com/retrieve/pii/S0896627300812106) 1050
.com/retrieve/pii/S0896627300812106 doi: 10.1016/S0896-6273(00)81210-6 1051
- Wall, M. B., & Smith, A. T. (2008, February). The Representation of Egomotion in 1052
the Human Brain. *Current Biology*, 18(3), 191–194. Retrieved 2020-07-20, from 1053
<https://linkinghub.elsevier.com/retrieve/pii/S0960982207024852> doi: 1054
10.1016/j.cub.2007.12.053 1055
- Wann, J., & Land, M. (2000, August). Steering with or without the flow: is the 1056
retrieval of heading necessary? *Trends in Cognitive Sciences*, 4(8), 319–324. 1057
Retrieved 2020-07-18, from [https://linkinghub.elsevier.com/retrieve/](https://linkinghub.elsevier.com/retrieve/pii/S1364661300015138) 1058
pii/S1364661300015138 doi: 10.1016/S1364-6613(00)01513-8 1059
- Warren, W. H. (1988). Action Modes and Laws of Control for the Visual Guidance 1060
Of Action. In *Advances in Psychology* (Vol. 50, pp. 339–379). Elsevier. Re- 1061
trieved 2020-07-18, from [https://linkinghub.elsevier.com/retrieve/pii/](https://linkinghub.elsevier.com/retrieve/pii/S0166411508625649) 1062
S0166411508625649 doi: 10.1016/S0166-4115(08)62564-9 1063
- Warren, W. H. (2006). The dynamics of perception and action. *Psychological Review*, 1064
113(2), 358–389. Retrieved 2020-08-03, from [http://doi.apa.org/getdoi.cfm](http://doi.apa.org/getdoi.cfm?doi=10.1037/0033-295X.113.2.358) 1065
?doi=10.1037/0033-295X.113.2.358 doi: 10.1037/0033-295X.113.2.358 1066
- Warren, W. H. (2007). Action-scaled information for the visual control of locomotion. 1067
In *Closing the gap: The scientific writings of David N. Lee* (pp. 243–258). 1068
Erlbaum. 1069
- Warren, W. H., & Hannon, D. J. (1990, January). Eye movements and optical flow. 1070
Journal of the Optical Society of America A, 7(1), 160. Retrieved 2020-07-18, 1071
from <https://www.osapublishing.org/abstract.cfm?URI=josaa-7-1-160> 1072
doi: 10.1364/JOSAA.7.000160 1073
- Warren, W. H., Kay, B. A., & Yilmaz, E. H. (1996). Visual control of posture during 1074
walking: Functional specificity. *Journal of Experimental Psychology: Human* 1075
Perception and Performance, 22(4), 818–838. (Place: US Publisher: American 1076
Psychological Association) doi: 10.1037/0096-1523.22.4.818 1077
- Warren, W. H., Kay, B. A., Zosh, W. D., Duchon, A. P., & Sahuc, S. (2001, February). 1078
Optic flow is used to control human walking. *Nature Neuroscience*, 4(2), 213– 1079
216. Retrieved 2020-07-18, from <http://www.nature.com/articles/nn0201.213> 1080
doi: 10.1038/84054 1081
- Weinzaepfel, P., Revaud, J., Harchaoui, Z., & Schmid, C. (2013, December). DeepFlow: 1082
Large Displacement Optical Flow with Deep Matching. In *2013 IEEE Interna-* 1083
tional Conference on Computer Vision (pp. 1385–1392). Sydney, Australia: IEEE. 1084
Retrieved 2020-07-18, from <http://ieeexplore.ieee.org/document/6751282/> 1085
doi: 10.1109/ICCV.2013.175 1086
- Yu, X., Hou, H., Spillmann, L., & Gu, Y. (2017, January). Causal Evidence of Motion 1087
Signals in Macaque Middle Temporal Area Weighted-Pooled for Global Heading 1088
Perception. *Cerebral Cortex*, cercor;bh402v1. Retrieved 2020-07-20, from 1089

<https://academic.oup.com/cercor/article-lookup/doi/10.1093/cercor/bhw402> doi: 10.1093/cercor/bhw402 1090

Zajac, F. E., Neptune, R. R., & Kautz, S. A. (2002, December). Biomechanics and muscle coordination of human walking. *Gait & Posture*, 16(3), 215–232. Retrieved 2020-07-18, from <https://linkinghub.elsevier.com/retrieve/pii/S0966636202000681> doi: 10.1016/S0966-6362(02)00068-1 1091
1092
1093
1094
1095

Author Manuscript Draft